RESEARCH ARTICLE

Mathematical Modeling and *NSFD* Numerical Investigation of Rabies Transmission Dynamics with Immigration Factors

Hazrat Younas[1], **Imtiaz Ahmad**[1,*], **Naseer Ul Haq**[1], **Azizur Rahman**[1] **and Hanif Ullah**[1]

[1] Department of Mathematics, University of Malakand, Chakdara 18000, Khyber Pakhtunkhwa, Pakistan

Abstract

In this study, a compartmental mathematical model is developed to study the rabies transmission process from dog to human. The model consists of eight compartments: susceptible, exposed, infected, recovered groups for dogs and humans $(S_D, E_D, I_D, R_D, S_H, E_H, I_H, R_H)$. The basic reproduction number R_0 is derived, and sensitivity analysis is performed to identify the most influential epidemiological parameters. Disease-free equilibrium stability analysis is also carried out to identify the conditions for rabies eradication. One of the main goals of this work is to compare the disease dynamics in vaccinated and unvaccinated cases, which is carried out with the support of numerical simulations. Both the fourth-order Runge–Kutta (RK4) and Nonstandard Finite Difference (NSFD) methods are used to solve the system. Numerical simulations demonstrate that vaccination substantially reduces the infected populations and increases the partially immune populations in both species. Furthermore, the importance of the transmission rate β_{DH} of the dog to human transmission is explored to gain insight into the role of this transmission route in the incidence of human rabies. In general, the results point to vaccination as a very potent control measure and show that NSFD method maintains the qualitative features of the system and yields results similar to the classical RK4 method.

Keywords: rabies, stability analysis, RK-4 vs NSFD method.

1 Introduction

Rabies is a fatal zoonotic viral disease of the central nervous system (CNS) caused by the Lyssavirus genus (Rhabdoviridae, order Mononegavirales) that leads to severe CNS damage and frequently death. Mathematical models have been developed to study the impact of vaccination and infectious immigrants on rabies transmission and public health outcomes [1]. The virus quickly travels up the neural pathways to the brain and, when clinical signs are seen, the disease is almost always fatal. Rabies is a major public health problem in the world, and has been found in over 150 countries and territories [2]. Domestic dogs are the primary reservoir of human infections in Asia,

Submitted: 24 July 2026
Revised: 28 August 2026
Accepted: 29 August 2026
Published: 30 September 2026

Vol. 3, **No.** 1, 2027.
10.62762/JNSPM.2026.292872

***Corresponding author:**
✉ Imtiaz Ahmad
mathskhan18@gmail.com

Citation
Younas, H., Ahmad, I., Ul Haq, N., Rahman, A., & Ullah, H. (2026). Mathematical Modeling and *NSFD* Numerical Investigation of Rabies Transmission Dynamics with Immigration Factors. *Journal of Numerical Simulations in Physics and Mathematics*, 3(1), 1–18.

Africa and Latin America, and foxes, skunks, bats and raccoons are the main reservoirs in the United States [3]. Rabies prevention remains challenging in endemic regions owing to limited access to canine vaccination, post-exposure prophylaxis, disease surveillance, and public health infrastructure. Pre-exposure prophylaxis (vaccination before exposure) and post-exposure (PEP) are both important in achieving good control of rabies. Novel mathematical approaches have been developed for analyzing rabies endemic dynamics and evaluating intervention strategies [4]. There has been a long history of mathematical modelling of rabies transmission dynamics and evaluation of control strategies. [5] conducted a scoping review of mathematical modelling and phylodynamic approaches used to study dog rabies dynamics and control strategies, synthesizing evidence on the effectiveness of vaccination and surveillance programs across multiple settings. [6] studied the global dynamics and numerical simulations of a vaccinated mathematical model for rabies, demonstrating the effectiveness of vaccination in reducing disease burden. [7] developed a mathematical model of dog rabies transmission dynamics and applied optimal control analysis to evaluate the effectiveness of vaccination and culling interventions, while [8] developed a mathematical model to assess the impact of contact rate and environmental factors on the transmission dynamics of rabies in both human and dog populations. [9] investigated fractional-order rabies models and obtained numerical solutions via Newton polynomial methods, demonstrating improved accuracy in capturing the memory effects inherent in rabies transmission dynamics. [10] analysed a time-delayed rabies model in human and dog populations, incorporating control measures to evaluate their impact on disease dynamics, whereas [11] provided a comprehensive review of mathematical models for rabies, summarizing key findings on transmission dynamics and the evaluation of control strategies including vaccination and post-exposure prophylaxis. Other work focused on strategic modeling of immunization: [12] applied a mathematical model to simulate the spread of the rabies virus, providing quantitative insights into transmission patterns and the effects of intervention measures, and [13] assessed the risk of rabies spread using mathematical modelling, evaluating the conditions under which the disease could re-establish in a previously rabies-free setting such as Japan. Fractional-order formulations have also been employed to examine stability, susceptibility, and vaccination impact in rabies models [14]. [15] employed the homotopy perturbation method to obtain analytic approximate solutions of the rabies transmission system, providing an alternative semi-analytical approach that avoids the need for optimal control formulations, while [16] applied optimal control theory to rabies epidemic management under resource-limited conditions in Nepal, identifying cost-effective vaccination strategies but leaving open certain questions about the practical limitations of these interventions; [17] analysed the transmission dynamics and control of rabies in China. At the global scale, [18] quantified the transmission dynamics and prospects for the elimination of canine rabies.

Based on these studies and in line with the objectives of Global Alliance for Rabies Control [19], this study develops a compartmental mathematical model incorporating vaccination and immigration factors. The model accounts for the limitations of vaccination and treatment in preventing rabies transmission among humans and dogs, and analyses its dynamics through stability analysis, sensitivity analysis, and numerical simulation using both RK4 and NSFD methods, aiming to provide insights into effective intervention strategies.

2 Model Formulation

We create a two-strata (human and dog) model for rabies virus transmission based on the model of [6]. The dog population is split into four compartments: the susceptible S_D, the exposed E_D, the infected I_D, and the partially immune R_D dogs. Thus, the total dog population is given by

$$N_D = S_D + E_D + I_D + R_D.$$

Likewise, human individuals are grouped into susceptible (S_H), exposed (E_H), infected (I_H), and partially immune (R_H) compartments such that the total number of human individuals at any given time is

$$N_H = S_H + E_H + I_H + R_H.$$

Direct transmission of rabies occurs from infected dogs to susceptible dogs and from infected dogs to susceptible humans. No human-to-human transmission is considered.

The susceptible dog population, S_D, is increased by recruitment at a rate of A_D. We let δ_D represent the rate at which exposed dogs move from the exposed compartment to the infected or recovered

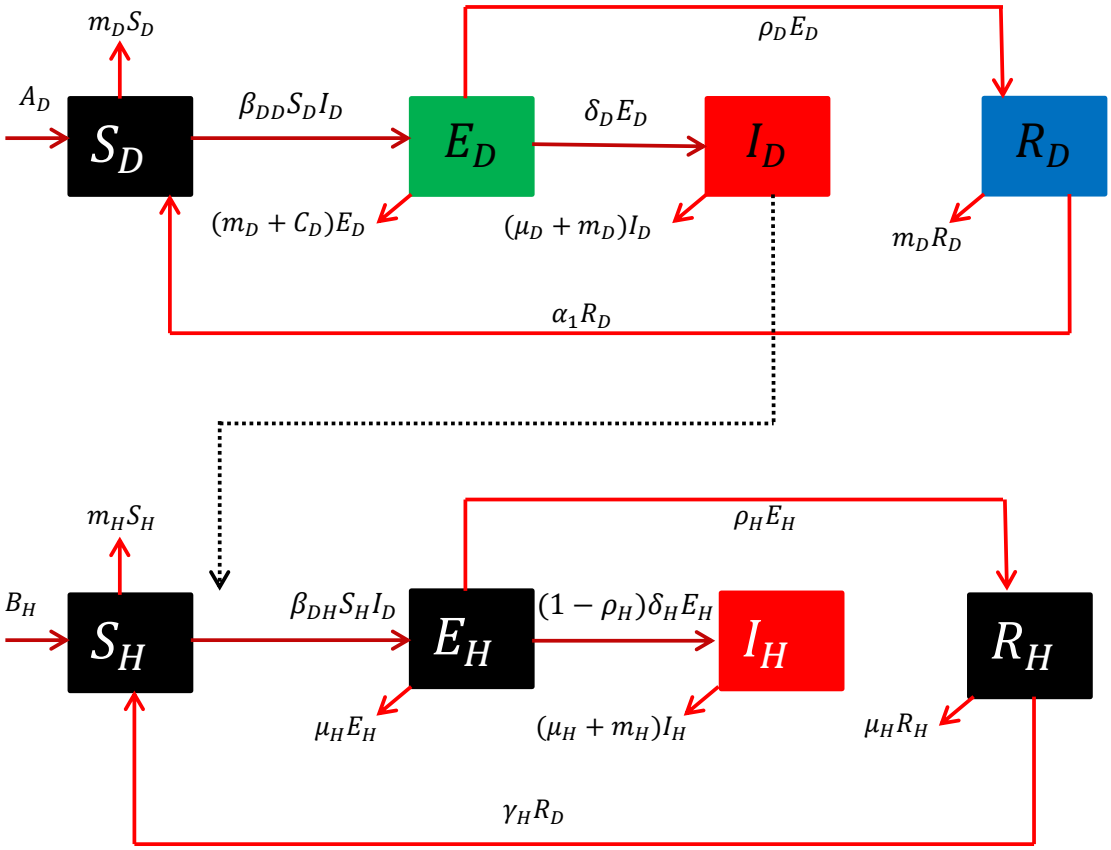

Figure 1. Flow-Chart of the proposed model.

compartments, and let α_1 represent the rate at which partially immune dogs lose their immunity and become exposed again. In dogs, the failure rate of pre-exposure prophylaxis is $1-\rho_H$, while the rates of natural death and disease-induced death are μ_D and m_D, respectively.

The susceptible human population, S_H, is increased by births or immigration at a rate of B_H. The transmission and contact rate from infected dogs to susceptible humans is denoted by β_{DH}. The parameter γ_H represents the rate at which humans lose immunity, while δ_H represents the transition rate of exposed humans to the infected or recovered compartments. The natural death rate and rabies-induced death rate in humans are denoted by μ_H and m_H, respectively. After clinical signs of rabies occur, natural recovery is considered impossible. Post-vaccination and natural immunity are limited and become lifelong only after some time.

The model also incorporates the effect of individuals entering the population from outside the infected population. In particular, exposed and infected dogs (or humans) may be recruited into the population at a rate Λ_I. This term represents the external introduction of the rabies virus, which may maintain the infection cycle even after local transmission has been controlled.

$$\begin{cases} \frac{dS_D}{dt} = A_D + \alpha_1 R_D - (m_D + \beta_{DD} I_D) S_D, \\ \frac{dE_D}{dt} = \beta_{DD} I_D S_D - \delta_D E_D - \rho_D E_D - (m_D + C_D) E_D, \\ \frac{dI_D}{dt} = \delta_D E_D - (\mu_D + m_D) I_D, \\ \frac{dR_D}{dt} = \rho_D E_D - (\alpha_1 + m_D) R_D, \\ \frac{dS_H}{dt} = B_H + \gamma_H R_H - (m_H + \beta_{DH} I_D) S_H, \\ \frac{dE_H}{dt} = \beta_{DH} S_H I_D - (m_H + \rho_H E_H + (1-\rho_H) S_H) E_H, \\ \frac{dI_H}{dt} = (1-\rho_H)\delta_H E_H - (\mu_H + m_H) I_H, \\ \frac{dR_H}{dt} = \rho_H E_H - m_H R_H - \gamma_H R_H. \end{cases} \tag{1}$$

Initial conditions are given below:

$$S_D(0) > 0, E_D(0) \geq 0, I_D(0) \geq 0, R_D(0) \geq 0,$$
$$S_H(0) \geq 0, E_H(0) \geq 0, I_H(0) \geq 0. R_H(0) \geq 0,$$

The proposed model is illustrated in Figure 1.

3 Positivity of the Solutions

It is necessary to demonstrate that all of the state variable parameters are non-negative as model (1) represents the animal population. We show that all state variables remain nonnegative for all$t, \geq 0$.

3.1 Boundedness of the Model

Theorem 1: *Consider the rabies transmission model 1, then, for every nonnegative initial condition, the solutions remain nonnegative and are uniformly bounded for all* $t \geq 0$.
proof Let the total population of dogs

$$N_D = S_D + E_D + I_D + R_D$$

be the total dog population. Differentiating with respect to time gives

$$\frac{dN_D}{dt} = \frac{dS_D}{dt} + \frac{dE_D}{dt} + \frac{dI_D}{dt} + \frac{dR_D}{dt}.$$

Substituting the corresponding equations, we obtain

$$\begin{aligned}\frac{dN_D}{dt} &= A_D + \alpha_1 R_D - (m_D + \beta_D I_D)S_D \\ &+ \beta_D I_D S_D - (\delta_D + \rho_D + m_D + C_D)E_D \\ &+ \delta_D E_D - (\mu_D + m_D)I_D \\ &+ \rho_D E_D - (\alpha_1 + m_D)R_D.\end{aligned}$$

After cancellation of the transmission and transition terms, we get

$$\frac{dN_D}{dt} = A_D - m_D S_D - (m_D + C_D)E_D - (\mu_D + m_D)I_D - m_D R_D.$$

Since $C_D > 0$ and $\mu_D > 0$, it follows that

$$\frac{dN_D}{dt} \leq A_D - m_D(S_D + E_D + I_D + R_D).$$

$$\frac{dN_D}{dt} \leq A_D - m_D N_D.$$

By the comparison theorem,

$$N_D(t) \leq N_D(0)e^{-m_D t} + \frac{A_D}{m_D}\left(1 - e^{-m_D t}\right).$$

$$\limsup_{t\to\infty} N_D(t) \leq \frac{A_D}{m_D}.$$

$$N_H = S_H + E_H + I_H + R_H$$

be the total human population. Then

$$\frac{dN_H}{dt} = \frac{dS_H}{dt} + \frac{dE_H}{dt} + \frac{dI_H}{dt} + \frac{dR_H}{dt}.$$

Substituting the model equations gives

$$\begin{aligned}\frac{dN_H}{dt} &= B_H + \gamma_H R_H - (m_H + \beta_{DH} I_D)S_H \\ &+ \beta_{DH} S_H I_D - (m_H + \rho_H \delta_H + (1 - \rho_H)\delta_H)E_H \\ &+ (1 - \rho_H)\delta_H E_H - (\mu_H + m_H)I_H \\ &+ \rho_H E_H - (m_H + \gamma_H)R_H.\end{aligned}$$

$$\frac{dN_H}{dt} \leq B_H - m_H N_H.$$

Again, by the comparison theorem,

$$N_H(t) \leq N_H(0)e^{-m_H t} + \frac{B_H}{m_H}\left(1 - e^{-m_H t}\right).$$

Consequently,

$$\limsup_{t\to\infty} N_H(t) \leq \frac{B_H}{m_H}.$$

Hence, all solutions enter the positively invariant region

$$\Omega = \left\{(S_D, E_D, I_D, R_D, S_H, E_H, I_H, R_H) \in \mathbb{R}^8_+ : \right.$$
$$\left. N_D \leq \frac{A_D}{m_D}, \qquad N_H \leq \frac{B_H}{m_H}\right\}.$$

Therefore, the rabies transmission model is biologically well posed, and all solutions remain positive and bounded for all $t \geq 0$.

4 Equilibrium Point

4.1 Disease-Free Equilibrium Point

With the condition that there is no rabies infection in either of the two populations, we set the infected and exposed compartments equal to zero, that is, $E_D = 0, I_D = 0, E_H = 0$, and $I_H = 0$. Plugging these into system (1) and solving the associated algebraic equations, we get the disease-free equilibrium (DFE) that is the steady-state of the system when there is no transmission of rabies at all. The condition of this balance is used as the starting point to study the local and global stability of the model as well as to calculate the threshold condition for disease invasion. Hence, the *DFE* is denoted by $E_0 = (S_D^0, E_D^0, I_D^0, R_D^0, S_H^0, E_H^0, I_H^0, R_H^0)$, is given by:

$$E_0 = \left(\frac{A_D}{m_D}, 0, 0, 0, \frac{B_H}{m_H}, 0, 0, 0\right)$$

5 Endemic Equilibrium Point

The endemic equilibrium state of a mathematical epidemic model is the state of disease being constantly positive over time. The endemic equilibrium has infected individuals present, $((I > 0))$ unlike the disease-free equilibrium. At this point, the rates of new infections, recovery, recruitment, and natural or disease-related deaths are balanced, so the sizes of all compartments remain unchanged with time. The endemic equilibrium solution is the point where all the time derivatives in the model are equal to zero and the algebraic equations can be solved for while keeping the infected compartment positive. Typically, the existence of this equilibrium is a function of the basic reproduction number R_0. For the majority of epidemic models, the endemic equilibrium will only occur if, $(R_0 > 1)$, meaning that, on average, more than one secondary infection will be produced by an infected individual. This condition permits the disease to persist in the population. The endemic equilibrium is significant because it could be used to get information about the long-term dynamics of the disease and to assess the effectiveness of various control measures such as vaccination, treatment, quarantine, or reducing the transmission rate. Stability analysis of the endemic equilibrium decides whether or not the disease is at the endemic level or whether the system will have small perturbations that will cause the system to move away from the endemic equilibrium.

$$\begin{cases} S_D^* = \left(\frac{(m_H+\gamma_H)A_D+\alpha_1\rho_H E_H^*}{(m_D+B_D I_D^*)(m_H+\gamma_H)}\right) \\ E_D^* = \frac{B_H S_D^* I_D^*}{(\delta_D\rho_D+m_D+C_D)} \\ I_D^* = \frac{\delta_D E_D^*}{(\mu_D+m_D)}, \\ R_D^* = \frac{\rho_D}{(\alpha_1+m_D)}\frac{B_D S_D^* I_D^*}{(\delta_D\rho_D+m_D+C_D)}, \\ S_H^* = \frac{B_H+\gamma_H R_H^*}{(m_H+B_{DH} I_H^*)}, \\ I_H^* = \frac{(1-\rho_H)\delta_H E_H^*}{(\mu_H+m_H)}, \\ E_H^* = \frac{\beta_{DH} S_H^* I_H^*}{(m_H+\rho_H+(1-\rho_H)\delta_H)}, \\ R_H^* = \frac{\rho_H\beta_{DH} S_H^* I_H^*}{(m_H+\rho_H+(1-\rho_H)\delta_H)(m_H+\gamma_H)}, \end{cases}$$

Note that if $R_0 < 1$, only the disease-free equilibrium exists and is stable; if $R_0 = 1$, a bifurcation occurs at the threshold; if $R_0 > 1$, the disease-free equilibrium becomes unstable and a unique endemic equilibrium exists.

6 Basic Reproduction Number R_0

In this scenario R_0 is the expected number of new infections that can be generated in a fully susceptible population of dogs and humans (see also [20]). Given this change of infected compartments we refer to our compartments as the E_D, I_D, E_H, and I_H compartments, we can now construct the next generation matrix (NGM) operator. This approach offers a structured way of quantifying the transmission potential of rabies in the inter-human and intra-dog system. The threshold parameter R_0 is the value of the disease parameter which indicates whether the disease will spread and be sustained in the population. Specifically, when the value of R_0 is less than 1, then the average number of secondary infections produced by every infected person will be less than one, which means that eventually the rabies will be eliminated. If $R_0 > 1$ on the other hand, the infection spreads via the susceptible population and can become endemic. We now write the class of the model system that is infected (1).

$$\begin{cases} \frac{dE_D}{dt} = \beta_D I_D S_D - \delta_D E_D - \rho_D E_D - (m_D + C_D)E_D, \\ \frac{dI_D}{dt} = \delta_D E_D - (\mu_D + m_D)I_D, \\ \frac{dE_H}{dt} = \beta_{DH} S_H I_D - (m_H + \rho_H E_H + (1-\rho_H)S_H)E_H, \\ \frac{dI_H}{dt} = (1-\rho_H)\delta_H E_H - (\mu_H + m_H)I_H, \end{cases}$$

$$F = \begin{pmatrix} \beta_{DD} I_D S_D \\ 0 \\ \beta_{DH} S_H I_D \\ 0 \end{pmatrix},$$

$$V = \begin{pmatrix} \delta_D E_D + \rho_D E_D + (m_D + C_D)E_D \\ (\mu_D + m_D)I_D - \delta_D E_D \\ m_H + \rho_H + (1-\rho_H)E_H \\ (\mu_H + m_H)I_H - (1-\rho_H)\delta_H E_H \end{pmatrix},$$

$$F^* = \begin{pmatrix} 0 & \beta_{DD} S_D^0 & 0 & 0 \\ 0 & 0 & 0 & 0 \\ 0 & 0 & 0 & \beta_{Dh} S_H^0 \\ 0 & 0 & 0 & 0 \end{pmatrix},$$

$$V^{*-1} = \begin{pmatrix} B & 0 & 0 & 0 \\ B_1 & \frac{1}{m_D + \mu_D} & 0 & 0 \\ 0 & 0 & \frac{1}{B_2} & 0 \\ 0 & 0 & B_3 & \frac{1}{m_H + \mu_H} \end{pmatrix}, \quad (2)$$

$$B_1 = \frac{m_H\delta_D - S_H^0\delta_H - S_H^0\delta_D\rho_H}{(m_D + \mu_D)(C_D + m_D + \delta_D + \rho_D)B_2}, \quad (3)$$

$$B_2 = m_H + S_H^0(1-\rho_H) + \rho_H, \quad (4)$$

$$B_3 = \frac{\beta_{DH} S_H^0 \delta_H (1-\rho_H)}{(m_H + \mu_H)B_2}. \quad (5)$$

$$FV^{*-1} = \begin{pmatrix} Z_1 & \frac{\beta_{DH} A_D}{m_D(m_D+\mu_D)} & 0 & 0 \\ 0 & 0 & 0 & 0 \\ 0 & 0 & Z_2 & \frac{\beta_{DH} B_H}{m_H(m_H+\mu_H)} \\ 0 & 0 & 0 & 0 \end{pmatrix} \tag{6}$$

$$Z_1 = \frac{\beta_D S_D^0 \left(m_H \delta_D - S_H^0 \delta_H - S_H^0 \delta_D \rho_H\right)}{(m_D+\mu_D)(C_D+m_D+\delta_D+\rho_D)B_2}, \tag{7}$$

$$Z_2 = \frac{\beta_{DH} S_D^0 \delta_D (\rho_H - 1)}{(m_H+\mu_H)B_2}. \tag{8}$$

$$B = \frac{1}{C_D + m_D \delta_D + \rho_D} \tag{9}$$

$$R_0 = \frac{B_H A_D (m_H + \delta_D \delta_H - \delta_D \rho_H)}{m_D m_H (m_D+\mu_D) B_4 (m_H + A_H(1-\rho_H) + \rho_H)}, \tag{10}$$

where

$$B_4 = C_D + m_D + \delta_D + \rho_D.$$

Figure 2 illustrates the behaviour of R_0 as a function of key epidemiological parameters. Panel (a) shows that R_0 increases with the human recruitment rate B_H and decreases with the dog natural mortality rate m_D, indicating that larger susceptible populations and lower mortality promote disease spread. Panel (b) demonstrates a positive relationship between R_0 and the dog disease progression rate δ_D: faster progression from exposed to infectious dogs amplifies transmission potential. Panel (c) confirms that R_0 scales proportionally with the dog recruitment rate A_D, since a larger dog population provides more opportunities for transmission. Panel (d) presents the overall R_0 surface, highlighting the joint sensitivity to these parameters. These findings underscore the importance of dog population management and vaccination campaigns in reducing R_0 below the critical threshold of unity, and confirm the value of sensitivity analysis for identifying leverage points in rabies control strategies.

7 Sensitivity Analysis of R_0

The fundamental reproduction number R_0 of the model is examined through a sensitivity analysis of the model parameters in it. This research looks closely at the most relevant factors which interfere in the spread and control of rabies in dog and human cases. We explore the sensitivity of some important parameters in the rabies virus model (1) to see how sensitive they are when it comes to the value of R_0. This helps to understand which epidemiological parameters are most important and thus should be targeted in the development of an effective prevention and control strategy. The sensitivity indices can be calculated using the technique proposed in [21]. The standard sensitivity index of R_0 is given by:

$$Z_\theta^{R_0} = \frac{\partial R_0}{\partial \theta} \times \frac{\theta}{R_0}, \tag{11}$$

where $\theta \in \{B_H, A_D, \delta_D, \delta_H, \rho_H, \rho_D, m_D, m_H, \mu_D, C_D, \alpha_1\}$

$$\begin{cases} Z_{(B_H)}^{(R_0)} = \left(\frac{\partial R_0}{\partial B_H} \times \frac{B_H}{R_0}\right) = 1, \\ Z_{(A_D)}^{(R_0)} = \left(\frac{\partial R_0}{\partial A_D} \times \frac{A_D}{R_0}\right) = 1, \\ Z_{(m_H)}^{(R_0)} = \left(\frac{\partial R_0}{\partial m_H} \times \frac{m_H}{R_0}\right) = \frac{-\left(-\delta_D A_H(\rho_H-1)(\delta_H-\rho_H)+\delta_D(\delta_H-\rho_H)(2m_H+\rho_H)+m_H^2\right)}{(-A_H(\rho_H-1)+m_H+\rho_H)(\delta_D(\delta_H-\rho_H)+m_H)} \\ Z_{(\delta_D)}^{(R_0)} = \left(\frac{\partial R_0}{\partial \delta_D} \times \frac{\delta_D}{R_0}\right) = \frac{\delta_D(C_D(\delta_H-\rho_H)+\delta_H(m_D+\rho_D)-m_D\rho_H-\rho_D\rho_H-m_H)}{(C_D+\delta_D+m_D+\rho_D)(\delta_D(\delta_H-\rho_H)+m_H)} \\ Z_{(\delta_H)}^{(R_0)} = \left(\frac{\partial R_0}{\partial \delta_H} \times \frac{\delta_H}{R_0}\right) = \frac{\delta_D\delta_H}{-\delta_D\rho_H+\delta_D\delta_H+m_H} \\ Z_{(\rho_H)}^{(R_0)} = \left(\frac{\partial R_0}{\partial \rho_H} \times \frac{\rho_H}{R_0}\right) = \frac{\rho_H(A_H(\delta_D(\delta_H-1)+m_H)-\delta_D(\delta_H+m_H)-m_H)}{(-A_H(\rho_H-1)+m_H+\rho_H)(\delta_D(\delta_H-\rho_H)+m_H)} \\ Z_{(m_D)}^{(R_0)} = \left(\frac{\partial R_0}{\partial m_D} \times \frac{m_D}{R_0}\right) = \frac{-(C_D(\mu_D+2m_D)+\delta_D X_1+2\mu_D m_D+\mu_D\rho_D+2m_D\rho_D+3m_D^2)}{(\mu_D+m_D)(C_D+\delta_D+m_D+\rho_D)} \\ X_1 = (\mu_D+2m_D)Z_{(\mu_D)}^{(R_0)} = \left(\frac{\partial R_0}{\partial \mu_D} \times \frac{\mu_D}{R_0}\right) = \frac{-\mu_D}{\mu_D+m_D} \\ Z_{(C_D)}^{(R_0)} = \left(\frac{\partial R_0}{\partial C_D} \times \frac{C_D}{R_0}\right) = \frac{-C_D}{C_D+\delta_D+m_D+\rho_D} \\ Z_{(\rho_D)}^{(R_0)} = \left(\frac{\partial R_0}{\partial \rho_D} \times \frac{\rho_D}{R_0}\right) = \frac{-\rho_D}{C_D+\delta_D+m_D+\rho_D} \\ Z_{(A_H)}^{(R_0)} = \left(\frac{\partial R_0}{\partial A_H} \times \frac{A_H}{R_0}\right) = \frac{-(A_H(1-\rho_H))}{A_H(1-\rho_H)+m_H+\rho_H} \end{cases}$$

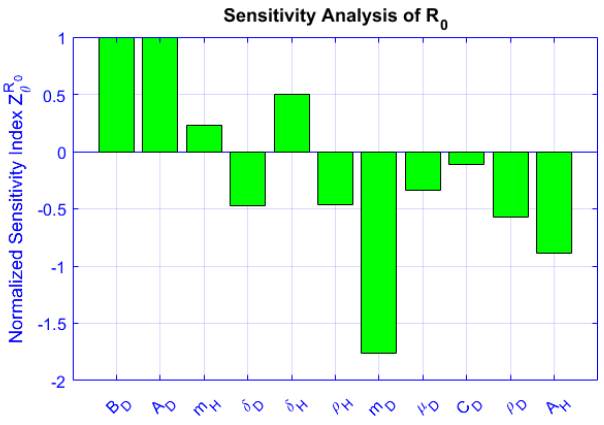

Figure 3. Normalized sensitivity indices of R_0 with respect to the model parameters.

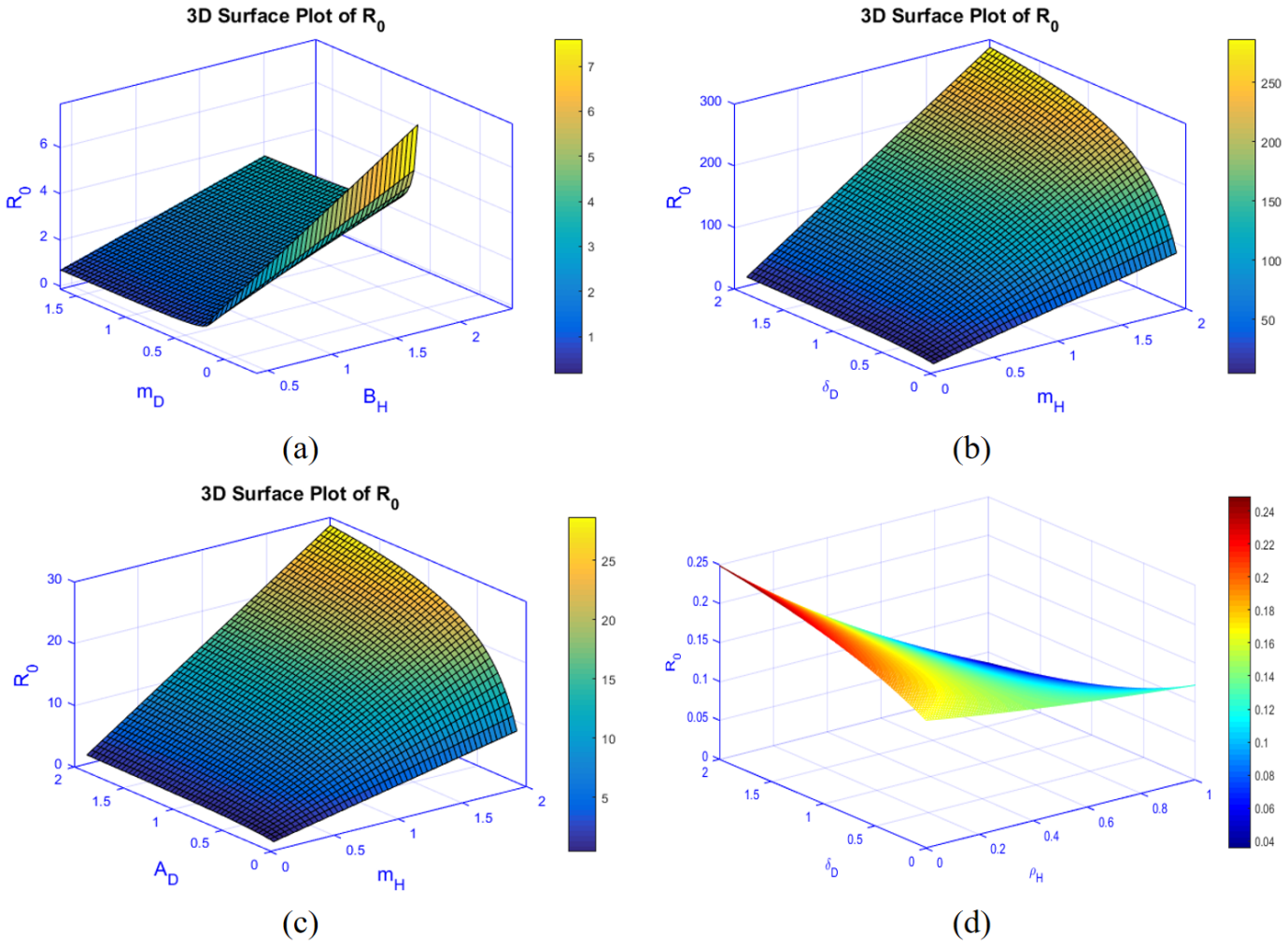

Figure 2. Behaviour of the basic reproduction number R_0 as a function of key epidemiological parameters: (a) R_0 versus the human recruitment rate B_H and dog mortality m_D, (b) R_0 versus the progression rate δ_D, (c) R_0 versus the dog recruitment rate A_D, and (d) the overall R_0 surface.

Discussion on Sensitivity Indices of R_0

The normalized sensitivity indices $Z_\theta^{R_0}$ measure the relative change in the basic reproduction number R_0 with respect to a proportional change in each parameter θ, and are summarized in Figure 3. A positive sensitivity index indicates that increasing the parameter will increase R_0, whereas a negative index implies that increasing the parameter will decrease R_0. The magnitude of the index reflects the strength of the influence. From the results, we observe that the parameters B_H (recruitment of susceptible humans) and A_D (recruitment of susceptible dogs) both have sensitivity indices equal to 1. This shows that they have a direct and proportional effect on R_0. A 10% increase in either of these parameters will result in a 10% increase in R_0. The mortality rates m_H (human) and m_D (dog) have negative sensitivity indices. This indicates that higher mortality in either population reduces R_0, since fewer individuals survive long enough to contribute to disease transmission. The disease progression rates δ_D and δ_H both have positive sensitivity indices. This suggests that faster progression from exposed to infectious classes increases R_0, thereby enhancing the spread of infection.The recovery fractions ρ_H (in humans) and ρ_D (in dogs) generally have negative sensitivity indices. This means that increasing recovery through treatment or immunity decreases R_0, thereby helping control the epidemic. The parameter C_D (dog control or culling) also has a negative sensitivity index, showing that increasing control efforts in dogs reduces R_0. The parameter A_H (related to human exposure to rabid dogs) shows a negative sensitivity index, implying that reducing contact between humans and infected dogs is beneficial for lowering R_0. Overall, the sensitivity analysis highlights that R_0 is most sensitive to recruitment parameters (B_H and A_D), followed by disease progression (δ_D,

δ_H), and control-related parameters (ρ_D, C_D, A_H). Effective strategies for reducing R_0 therefore include limiting the recruitment of susceptible hosts (e.g., dog population management), increasing recovery rates through vaccination or treatment, and strengthening dog control measures.

8 Local Stability at *DFE*

The disease-free equilibrium (DFE) is a condition of the system in which no individuals are infected and the disease cannot be sustained in the population. In the local sense, stability at the *DFE* is given by the basic reproduction number, and at this point, the behavior of the model can be analyzed to understand the stability and potential for disease outbreaks. If $R_0 < 1$ the *DFE* is locally asymptotically stable, otherwise unstable. The Jacobian matrix for the system (1) at E_0, is obtained as follows: $J(E_0) =$

$$\begin{pmatrix} A & 0 & A_1 & \alpha_1 & 0 & 0 & 0 & 0 \\ 0 & -A_2 & A_1 & 0 & 0 & 0 & 0 & 0 \\ 0 & S_D^0 & -A_3 & 0 & 0 & 0 & 0 & 0 \\ 0 & \rho_D & 0 & -A_4 & 0 & 0 & 0 & 0 \\ 0 & 0 & 0 & 0 & -m_H & 0 & A_5 & \gamma_H \\ 0 & 0 & 0 & 0 & 0 & -A_6 & A_7 & 0 \\ 0 & 0 & 0 & 0 & 0 & A_8 & -A_9 & 0 \\ 0 & 0 & 0 & 0 & 0 & \rho_H & 0 & -\gamma_H \end{pmatrix} \tag{12}$$

$$\begin{aligned} A_1 &= B_D S_D^0, \\ A_2 &= S_D^0 + \rho_D + m_D + C_D, \\ A_3 &= \mu_D + m_D, \\ A_4 &= \alpha_1 + m_D, \\ A_5 &= B_{DH} S_H^0, \\ A_6 &= m_H + \rho_H + (1-\rho_H)\delta_H, \\ A_7 &= B_H S_H^0, \\ A_8 &= (1-\rho_H)\delta_H, \\ A_9 &= \mu_H + m_H. \end{aligned}$$

We now show that the following result is important for the analysis of the local stability of the epidemic model at disease-free equilibrium.

Theorem: 2 *The proposed model system (1), is supposed to be LAS at* DFE *points, P_0 which is accommodated in the set Ω if $R_0 < 1$, whereas if $R_0 > 1$, the system is unstable.*
Proof: After the calculation we get the following eigenvalues of jacobian matrix $J(E_0)$, are obtained: $\lambda_1 = -a_1, \lambda_2 = -a_2, \lambda_3 = -B_H S_D^0 \lambda_4 = \delta_D a_2 a_4, \lambda_5 = -a_1 a_3, \lambda_6 = -m_H, \lambda_7 = -a_4, \lambda_8 = -a_6,$

Since $a_1, a_2 > 0$, we have $\lambda_1 = -a_1 < 0$ and $\lambda_2 = -a_2 < 0$. Since $B_H, S_D^0, \delta_D, a_2, a_4 > 0$, it follows that $\lambda_3 = -B_H S_D^0 \delta_D a_2 a_4 < 0$. The remaining eigenvalues $\lambda_4, \ldots, \lambda_8$ are also negative by similar arguments. Hence all eigenvalues of $J(E_0)$ are negative, confirming that E_0 is locally asymptotically stable when $R_0 < 1$. As a result, model (1) is LAS and all of the eigenvalues of the aforementioned Jacobian matrix are negative. There are no Rabies Virus in the host population, and the human population is in good health.

Theorem: 3 *In the feasible region, Ω the endemic equilibrium point E_1 of system (1) is globally asymptotically stable for $R_0 > 1$.*

proof. Suppose that $R_0 > 1$. Then the endemic equilibrium point

$$E_1 = (S_D^*, E_D^*, I_D^*, R_D^*, S_H^*, E_H^*, I_H^*, R_H^*)$$

exists. Consider the Lyapunov function

$$\begin{cases} \mathbb{V} = \frac{1}{2}[(S_D - S_D^*) + (E_D - E_D^*) + (I_D - I_D^*) \\ +(R_D - R_D^*)]^2 + \frac{1}{2}[(S_H - S_H^*) + (E_H - E_H^*) \\ +(I_H - I_H^*) + (R_H - R_H^*)]^2. \end{cases}$$

The function $\mathbb{V}$ is continuous, positive definite, and satisfies

$\mathbb{V}(E_1) = 0, \qquad \mathbb{V} > 0$ for all
$(S_D, E_D, I_D, R_D, S_H, E_H, I_H, R_H) \neq E_1.$

Differentiating (8) along the solutions of system (1) gives

$$\begin{aligned} \frac{d\mathbb{V}}{dt} =& \Big[(S_D - S_D^*) + (E_D - E_D^*) + (I_D - I_D^*) \\ &+ (R_D - R_D^*)\Big] \frac{d}{dt}(S_D + E_D + I_D + R_D) \\ &+ \Big[(S_H - S_H^*) + (E_H - E_H^*) + (I_H - I_H^*) \\ &+ (R_H - R_H^*)\Big] \frac{d}{dt}(S_H + E_H + I_H + R_H). \end{aligned}$$

Using system (1),

$\frac{d}{dt}(S_D+E_D+I_D+R_D) = A_D - m_D(S_D+E_D+I_D+R_D) - C_D E_D - \mu_D I_D,$

and

$\frac{d}{dt}(S_H+E_H+I_H+R_H) = B_H - m_H(S_H+E_H+I_H+R_H) - \mu_H I_H.$

Substituting these expressions into $\frac{d\mathbb{V}}{dt}$ and using the equilibrium relations satisfied by E_1, namely,

$$A_D = m_D(S_D^* + E_D^* + I_D^* + R_D^*) + C_D E_D^* + \mu_D I_D^*,$$

and

$$B_H = m_H(S_H^* + E_H^* + I_H^* + R_H^*) + \mu_H I_H^*,$$

it follows after simplification that

$$\frac{d\mathbb{V}}{dt} \leq 0,$$

with equality if and only if

$S_D = S_D^*,\ E_D = E_D^*,\ I_D = I_D^*,\ R_D = R_D^*,\ S_H = S_H^*,\ E_H = E_H^*,\ I_H = I_H^*,\ R_H = R_H^*.$

Hence, the largest invariant subset of

$$\left\{(S_D, E_D, I_D, R_D, S_H, E_H, I_H, R_H) \in \Omega : \frac{d\mathbb{V}}{dt} = 0\right\}$$

is the singleton $\{E_1\}$. By LaSalle's Invariance Principle, every solution with initial value in Ω converges to E_1 as $t \to \infty$. Hence, when $R_0 > 1$, the endemic equilibrium E_1 is globally asymptotically stable. Hence, when $R_0 > 1$ the endemic equilibrium point E_1 is globally asymptotically stable.

Theorem: 4 *The disease-free equilibrium point $E_0 = (P^0, 0)$ is globally asymptotically stable if $R_0 < 1$, and unstable if $R_0 > 1$.*

proof The rabies model system (1) can be written as. $p = (S_D, R_D, S_H, R_H), Q = (E_D, I_D, E_H, I_H$ and $E_0 = (\frac{A_D}{m_D}, 0, 0, 0, \frac{B_D H}{m_H},)$ Now, we have

$$\frac{dp}{dt} = \begin{pmatrix} A_D + a_1 R_D - (m_D + B_D I_D)\S_D \\ \rho_D E_D - (a_1 + m_D) R_D \\ B_H + \gamma R_H - (m_H + B_{DH} I_H) S_H \\ \rho_D E_H - m_H R_H - \gamma_H R_H \end{pmatrix}$$

At DFE Points

$$\frac{dp}{dt} = (P^0, 0) = \begin{pmatrix} A_D - \frac{m_D B_H H}{m_H} \\ 0 \\ B_D H \\ 0 \end{pmatrix}$$

$E_0(p^0, 0)$ has a unique equilibrium point $p^0 = \left(\frac{A_D}{m_D}, \frac{B_H}{m_H}\right)$ which is globally asymptotically stable. Hence, the condition (H1) hold p^0 several condition (H2) $G(P, Q)$=

$$\begin{pmatrix} A_D S_D I_D - \delta_D E_D - \rho_D E_D - (m_D + C_D) E_D \\ \delta_D E_D - (\mu_D + m_D) E_D \\ \beta_{DH} S_H I_H - ((m_H + \rho_H) + (1 - \rho_H)\delta) E_H \\ (1 - \rho_H)\delta_H E_H - (\mu_H + m_H) I_H \end{pmatrix}.$$

Then we get,

$$X = A_1(P^0, 0) = \begin{pmatrix} A_{11} & \beta_{DH} S_D^* & 0 & 0 \\ A_{12} & 0 & 0 & 0 \\ 0 & 0 & A_{13} & \beta_{DH} S_H \\ 0 & 0 & A_{14} & \end{pmatrix}.$$

where $A_{11} = -\delta_D - \rho_D - (m_D + C_D)$ $A_{12} = \delta_D - (\mu_D + m_D)$, $A_{13} = (m_H - \delta_H) + (1 - \rho_H)\delta_H$ $A_{14} = (1 - \rho_H)\delta_H - (\mu_H + m_H)$

It is now evident that the matrix X is an M-matrix, given that the elements off the diagonal are non-negative. Therefore, $XY - G(P, Q)$ equals $\hat{G}(P, Q)$.

$$\hat{G}(P, Q) = \begin{pmatrix} -N_1 & B_D S_D & 0 & 0 \\ N_2 & 0 & 0 & 0 \\ 0 & 0 & N_3 & \beta_{DH} \\ 0 & 0 & N_4 & \end{pmatrix} \begin{pmatrix} E_D \\ I_D \\ E_H \\ I_H \end{pmatrix}$$

$$- \begin{pmatrix} B_H S_D I_D - (\delta_D + \rho_D + (m_D + C_D)) E_D \\ \delta_D E_D - (\mu_D + m_D) E_D \\ B_{DH} S_H I_H - (m_H + \rho_H + (1 - \rho_H)\delta_H) E_H \\ (1 - \rho_H)\delta_H) E_H - (\mu_H + m_H) I_H \end{pmatrix}$$

Where $\delta_D - \rho_D - (m_D + C_d) = N_1, \delta_D - (\mu_D + m_D) = N_2, (m_H + \rho_H + (1 - \rho_H)\delta_H) = N_3,$
$(1 - \rho_H)\delta_H - (\mu_H + m_H) = N_4$

$$\hat{G}(P, Q) = \begin{pmatrix} B_D S_D^* - \delta_D - \rho_D - (m_D + C_D) \\ 0 \\ B_{DH} S_H^* - (m_H + \rho_H + (1 - \rho_H)\delta) \\ 0 \end{pmatrix}$$

Since it clear that $S_D^* > S_D$ and $S_H^* > S_H$ then it is clear That $\hat{G}(P, Q) \geq 0$, and $P^0 = \frac{A_D}{m_D}, \frac{B_{DH}}{m_H}$ is globally asymptotically Stable.

9 Bifurcation

In mathematical models, bifurcation can occur when the behavior of the model changes greatly due to small changes in the model's parameters. It gives the picture of system dynamics next to each of the

points of qualitative changes in the system evolution and enables them to grasp how the disease evolves for various conditions of the epidemic and the other parameters. Bifurcation analysis is useful for rabies transmission models in establishing whether the disease-free equilibrium is losing stability with as the increase in the transmission rate, and the emergence of an endemic equilibrium. In this analysis it is possible to obtain information about the threshold behaviour of the system as well as about long-term persistence or elimination of rabies. Investigation of the bifurcation which is occurring around the critical threshold allows us to interpret the conditions for the transition between eradication and persistence of the disease. We nuance our model at the threshold value $R_0 = 1$; we determine the parameter corresponding to the threshold value, namely β^*, and check the bifurcation which occurs at this point.

$$\beta^* = \frac{m_D m_H (m_D + \mu_D)(Q_1 + \rho_H)}{(m_H + \delta_D \delta_H - \delta_D \rho_H)}$$

where $Q_1 = C_D + m_D + \delta_D + \rho_D)(m_H + S_H(1 - \rho_H)$
The J matrix of the model (1) is given by:

$J(E^*) =$

$$\begin{pmatrix} -m_D & 0 & Q_2 & \alpha_1 & 0 & 0 & 0 & 0 \\ 0 & a_1 & Q_3 & 0 & 0 & 0 & 0 & 0 \\ 0 & S_D^* & -a_2 & 0 & 0 & 0 & 0 & 0 \\ 0 & \rho_D & 0 & -a_3 & 0 & 0 & 0 & 0 \\ 0 & 0 & 0 & 0 & -m_H & 0 & Q_4 & \gamma_H \\ 0 & 0 & 0 & 0 & 0 & -a_4 & B_H S_H^* & 0 \\ 0 & 0 & 0 & 0 & 0 & a_5 & -a_6 & 0 \\ 0 & 0 & 0 & 0 & 0 & \rho_H & 0 & -\gamma_H \end{pmatrix} \tag{13}$$

where $Q_2 = \beta_{DD} S_D^*, \quad Q_3 = \beta_{DD} S_D^*, \quad Q_4 = \beta_{DH} S_H^*$
After some computations, the eigenvalues of J_{E^*} are:

$\lambda_1 = -a_1,\ \lambda_2 = -a_2,\ \lambda_3 = -B_H S_D^*,\ \lambda_4 = \delta_D a_2 a_4,\ \lambda_5 = -a_1 a_3,\ \lambda_6 = -m_H,\ \lambda_7 = -a_4,\ \lambda_8 = -a_6$

All eigenvalues are negative real numbers, confirming stability. According to Castillo-Chavez and Song [22], we analyze the dynamics using the eigenvectors of J_{E^*}. We solve for the left and right eigenvectors to determine the types of bifurcations.

$J|0|(\beta^*)K = 0, \quad J =$

$$\begin{pmatrix} -m_D & 0 & Q_2 & \alpha_1 & 0 & 0 & 0 & 0 \\ 0 & a_1 & Q_3 & 0 & 0 & 0 & 0 & 0 \\ 0 & S_D^* & -a_2 & 0 & 0 & 0 & 0 & 0 \\ 0 & \rho_D & 0 & -a_3 & 0 & 0 & 0 & 0 \\ 0 & 0 & 0 & 0 & -m_H & 0 & Q_4 & \gamma_H \\ 0 & 0 & 0 & 0 & 0 & -a_4 & B_H S_H^* & 0 \\ 0 & 0 & 0 & 0 & 0 & a_5 & -a_6 & 0 \\ 0 & 0 & 0 & 0 & 0 & \rho_H & 0 & -\gamma_H \end{pmatrix} \tag{14}$$

The corresponding equations for the eigenvalues:

$$\begin{cases} -m_D K_1 + B_D S_D^* K_3 + \alpha_1 K_4 = 0 \\ a_1 K_2 + B_D S_D^* K_3 = 0 \\ \delta_D K_2 - a_2 K_3 = 0 \\ \rho_D K_2 - a_3 K_4 = 0 \\ -m_H K_5 + B_{DH} S_H^* K_7 + \gamma_H K_8 = 0 \\ -a_4 K_6 + B_H S_H^* K_7 = 0 \\ a_5 K_6 - a_6 K_7 = 0 \\ \rho_H K_6 - \gamma_H K_8 = 0 \end{cases}$$

Solving these, we find:

$K_1 = \frac{B_H S_D^* K_3 + \alpha_1 K_4}{m_D}, K_2 = \frac{B_H S_D^* K_3}{a_1}, K_3 = \frac{\delta_D K_2}{a_1}, K_4 = \frac{\rho_D K_2}{a_3}$,
$K_5 = \frac{\beta_{DH} S_H^* K_7 + \gamma_H K_8}{m_H}, K_6 = \frac{B_H S_H^* K_7}{a_4}, K_7 = \frac{a_5 K_6}{a_6}, K_8 = \frac{\rho_H K_6}{\gamma_H}$

The zero eigenvector on the left is

$$VJ^{|0|}(\beta^*) = 0$$

$$\begin{pmatrix} V_1 \\ V_2 \\ V_3 \\ V_4 \\ V_5 \\ V_6 \\ V_7 \\ V_8 \end{pmatrix}^T \cdot \begin{pmatrix} -m_D & 0 & Q_2 & \alpha_1 & 0 & 0 & 0 & 0 \\ 0 & a_1 & Q_3 & 0 & 0 & 0 & 0 & 0 \\ 0 & S_D^* & -a_2 & 0 & 0 & 0 & 0 & 0 \\ 0 & \rho_D & 0 & -a_3 & 0 & 0 & 0 & 0 \\ 0 & 0 & 0 & 0 & -m_H & 0 & Q_4 & \gamma_H \\ 0 & 0 & 0 & 0 & 0 & -a_4 & Q_5 & 0 \\ 0 & 0 & 0 & 0 & 0 & a_5 & -a_6 & 0 \\ 0 & 0 & 0 & 0 & 0 & \rho_H & 0 & -\gamma_H \end{pmatrix} \tag{15}$$

where

$$Q_5 = B_H S_H^* = \begin{pmatrix} 0 \\ 0 \\ 0 \\ 0 \\ 0 \\ 0 \\ 0 \\ 0 \end{pmatrix}$$

$$\begin{cases} -m_D K_1 = 0 \\ a_1 K_2 + \delta_D K_3 + \rho_D K_4 = 0 \\ B_D S_D^* K_3 + B_D S_D^* K_4 - a_2 = 0 \\ \alpha_1 K_1 - a_3 K_4 = 0 \\ -m_H K_5 = 0 \\ -a_4 K_6 + a_5 K_7 + \rho_H K_8 = 0 \\ \beta_{DH} S_H^* K_5 + B_H S_H^* K_6 - a_7 = 0 \\ \gamma_H K_5 - \gamma_H K_8 = 0 \end{cases}$$

After solving, we get $V_1 = V_4 = V_5 = V_6 = V_7 = V_8 = 0$.

To express the model (1) as $\frac{dg}{dt} = g(y)$ with $y = (y_1, y_2, \ldots, y_8)$ where $S_D = y_1$, $E_D = y_2$, $I_D = y_3$, $R_D = y_4$, $S_H = y_5$, $E_H = y_6$, $I_H = y_7$, $R_H = y_8$, we have:

$$\begin{cases} g_1 = A_D + \alpha_1 y_4 - (m_D + \beta_D y_3) y_1 \\ g_2 = \beta_D y_3 y_1 - (\delta_D + \rho_D + m_D + C_D) y_2 \\ g_3 = \delta_D y_2 - (m_D + m_H + \delta_H) y_3 \\ g_4 = \rho_D y_2 - (m_D + \alpha_1) y_4 \\ g_5 = A_H + \beta_{DH} y_7 - (m_H + B_H y_7) y_5 \\ g_6 = B_H y_7 y_5 - (\gamma_H + a_4) y_6 \\ g_7 = a_5 y_6 - (m_H + a_6) y_7 \\ g_8 = \rho_H y_6 - (m_H + a_7) y_8 \end{cases}$$

According to Castillo-Chavez and Song (2004) [22], the bifurcation functions can be established:

$$f_{100}(0, \beta^*) = 0, \qquad f_{110}(0, \beta^*) \neq 0,$$
$$f_{101}(0, \beta^*) \neq 0, \qquad f_{200}(0, \beta^*) \neq 0$$

Thus, a forward bifurcation is observed.

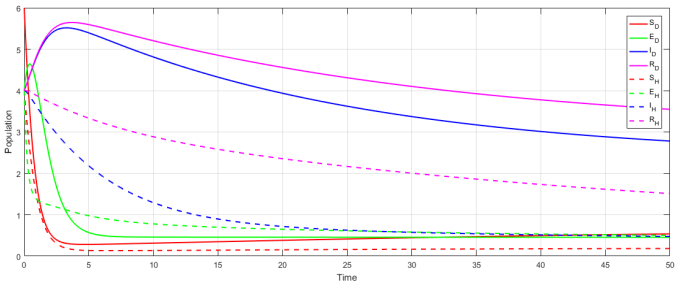

Figure 4. Evolution of animal and human populations over time.

10 Numerical Simulation

The numerical simulation in this section was done on MATLAB 2016a. The RK4 scheme was implemented using the built-in solver ODE45, while the NSFD scheme was implemented separately as a custom discretization following Mickens [23]. The dynamics of this rabies transmission model are well modeled by this solver. The following initial conditions are assumed for simulation: $S_D = 100, E_D = 4, I_D = 4, R_D = 4, S_H = 4, E_H = 4, I_H = 4, R_H = 4$. These are initial conditions that are set arbitrarily in order to generate model behavior that is representative. The model population dynamics with respect to rabies are presented in Figure 4. The results show that it doesn't take long for the number of susceptible animals to decrease to very low levels in the first few years. This reduction is mostly due to exposure to infected animals and so on susceptible animal population. Susceptibility gets less as animals come into contact with infected animals.

In line with the One Health approach, this graphical representation provides insight into the early impacts of rabies transmission. It also highlights the importance of vaccination strategies and infection control measures for effective rabies management.

From the result of the numerical simulation, shown in Figure 5, it is observed that the susceptible population (S) rises with time (Figure 5(a)), the infected population (I) decreases with time (Figure 5(c)), and the recovered population (R) increases with time (Figure 5(d)); the exposed class is shown in Figure 5(b). Moreover, the recovered population (R) cannot be less than I at any time (Figure 5(e)), which is consistent with the physical understanding of the problem.

Impact of β_{DH} on Rabies Transmission Dynamics

The impact of changing the transmission coefficient β_{DH}, that is, the probability of susceptible humans being infected from infected dogs, will be explored in this subsection. Several values of the model parameter β_{DH} were used, but the other model parameters were kept unchanged; the resulting human-compartment trajectories are collected in Figure 6. As seen in the time series of the susceptible human population ($S_H(t)$, Figure 6(a)), certain trends are important in disease dynamics. A higher value of β_{DH} leads to a more steep and quick reduction of the susceptible population of humans. This implies that the risk of exposure is also high when the transmission rate of the dog-to-human is increased, although only marginally, and hence the person is shifted to the "exposed" and then "infected" class. Similarly, as β_{DH} is increased, the number of exposed (E_H, Figure 6(c)) and infected humans (I_H, Figure 6(b)) will increase, which means that the transmitted infection is faster and more intense. The recovered human population (R_H, Figure 6(d)) initially rises as more people become infected and then recover. At higher levels of β_{DH}, however, R_H levels off or drops, possibly because of the high level of infection and the lack of recovery at a high level of transmission pressure. A threshold phenomenon is seen between $\beta_{DH} \approx 0.1, 0.03, 0.05, 0.07, 0.9$ where if the value of β_{DH} is

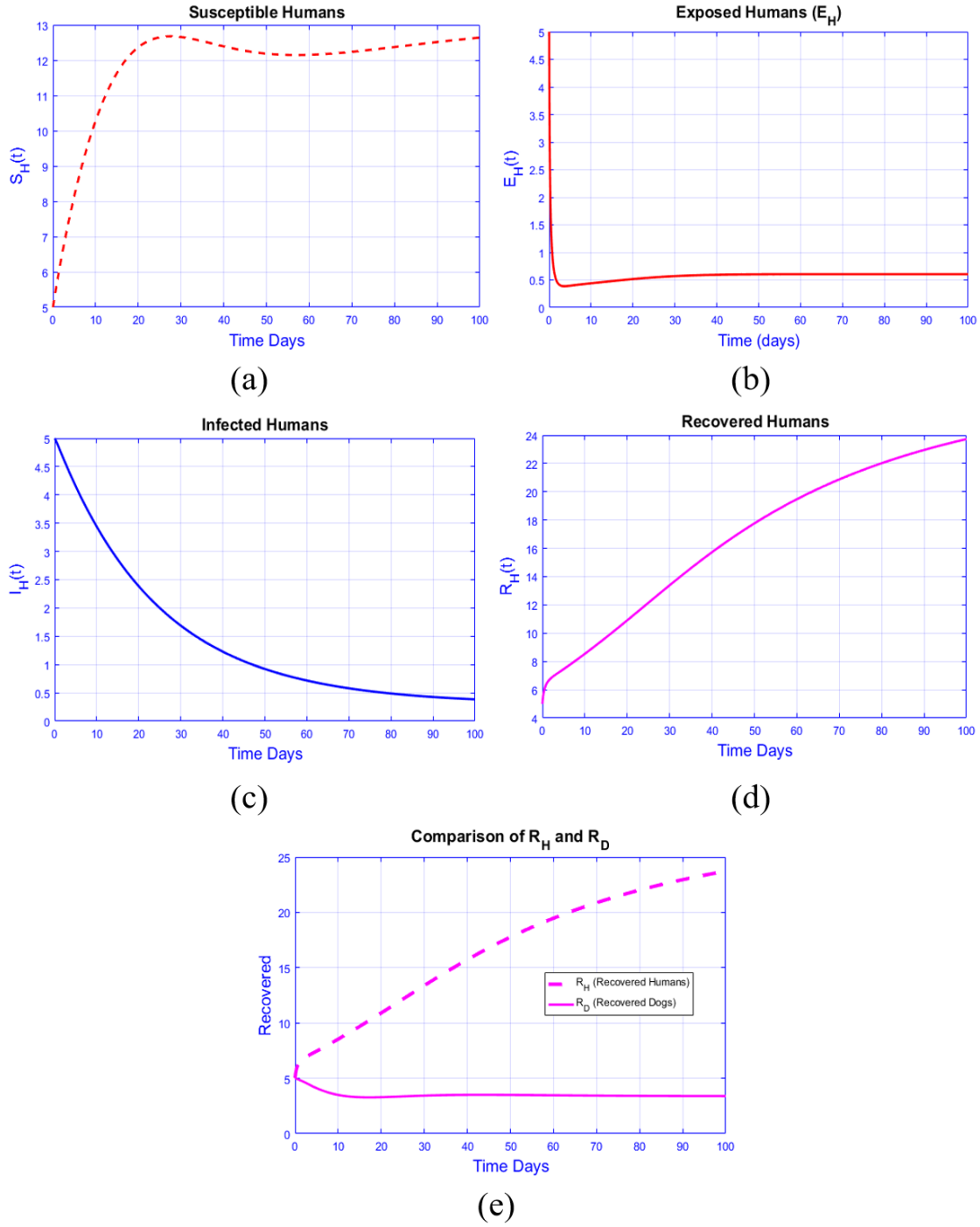

Figure 5. Time evolution of the human population compartments together with the recovered-class comparison: (a) susceptible S_H, (b) exposed E_H, (c) infected I_H, (d) recovered R_H, and (e) comparison of the recovered dog and human populations.

above this threshold level, it is seen that the system enters a quasi-endemic state with a persistent high level of infection. The observations demonstrate the importance of the dog-to-human route of transmission for the spread of rabies. Vaccination of dogs, dog population control, improved surveillance and public health education programs that limit human exposure to canines are effective ways to lower β_{DH}. As a result, such measures can be very important in controlling rabies and maintaining the vulnerable population in perpetuity.

As shown in Figure 7, in the presence of vaccination the number of infected individuals decreases significantly over time (Figure 7(b)), whereas in the absence of vaccination the number of infections continues to rise; the corresponding exposed class is shown in Figure 7(a). This demonstrates that vaccination is

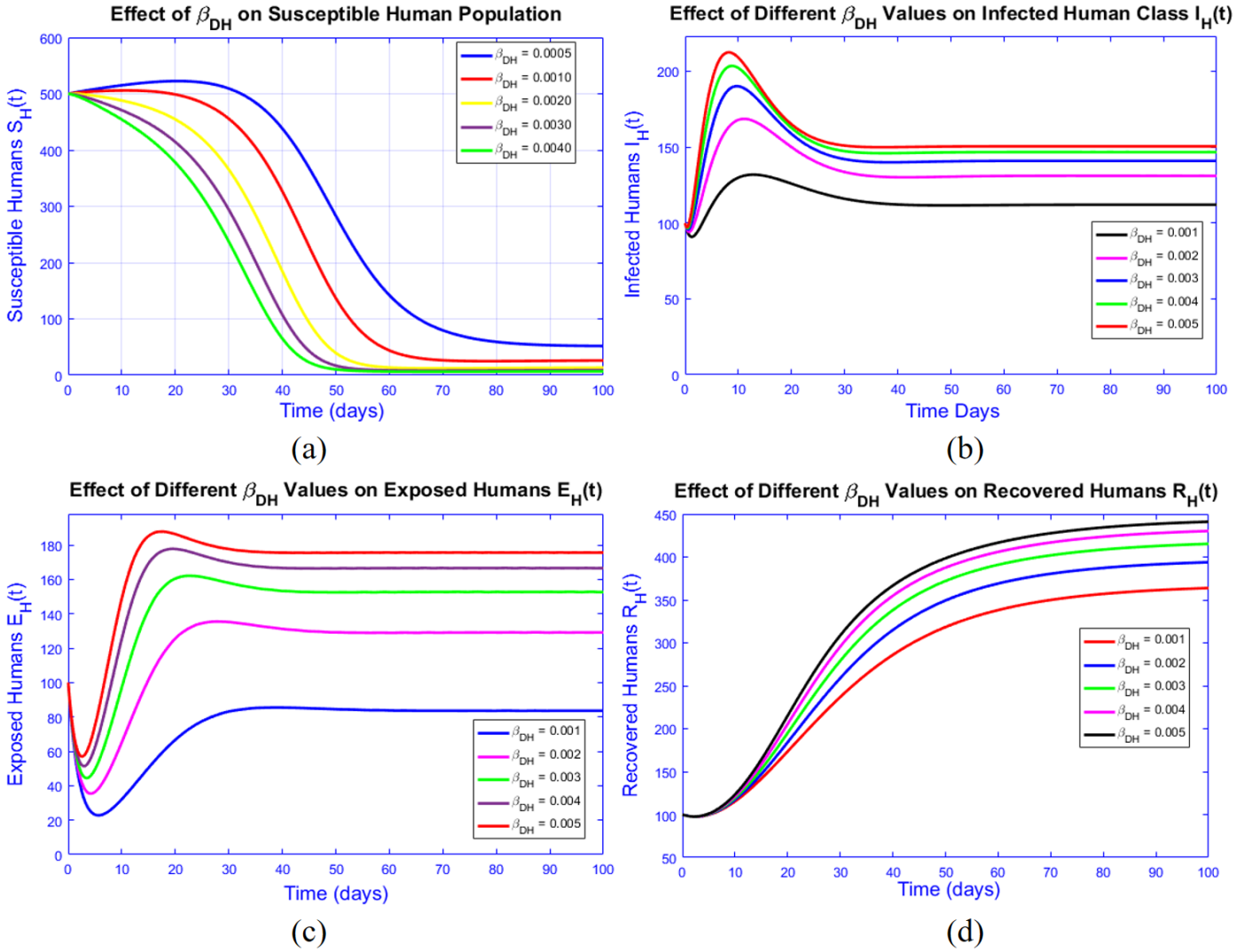

Figure 6. Effect of the dog-to-human transmission rate β_{DH} on the human compartments for several values of β_{DH}: (a) susceptible S_H, (b) infected I_H, (c) exposed E_H, and (d) recovered R_H.

essential in controlling the spread of rabies.

10.1 RK4 Scheme

The explicit RK4 numerical scheme is defined by:

$$
\begin{aligned}
k_1 &= h\left[A_D + \alpha_1 R_D^n - (m_D + \beta_D I_D^n) S_D^n\right],\\
w_1 &= h\left[\beta_D I_D^n S_D^n - (\delta_D + \rho_D + (m_D + C_D) E_D^n)\right],\\
m_1 &= h\left[\delta_D E_D^n - (\mu_D + m_D) I_D^n\right],\\
n_1 &= h\left[\rho_D E_D^n - (\alpha_1 + m_D) R_D^n\right],\\
o_1 &= h\left[B_D + \gamma_H R_H^n - (m_H + \beta_{DH} I_D^n) S_H^n\right],\\
p_1 &= h\left[\beta_{DH} S_H^n I_D^n - (m_H + \rho_H + (1-\rho_H)\delta_H) E_H^n\right],\\
q_1 &= h\left[(1-\rho_H)\delta_H E_H^n - (\mu_H + m_H) I_H^n\right],\\
j_1 &= h\left[\rho_H E_H^n - (\mu_H + \gamma_H) R_H^n\right],
\end{aligned}
$$

$$\downarrow$$

$$
\begin{aligned}
k_2 &= h\left[A_D + \alpha_1\left(R_D^n + \frac{n_1}{2}\right) - \left(m_D + \beta_D\left(I_D^n + \frac{m_1}{2}\right)\right)\right.\\
&\left.\left(S_D^n + \frac{k_1}{2}\right)\right],\\
w_2 &= h\left[\beta_D\left(I_D^n + \frac{m_1}{2}\right) W_1 - (\delta_D + \rho_D + m_D + C_D)\left(E_D^n + \frac{w_1}{2}\right)\right],\\
m_2 &= h\left[\delta_D\left(E_D^n + \frac{w_1}{2}\right) - (\mu_D + m_D)\left(I_D^n + \frac{m_1}{2}\right)\right],\\
n_2 &= h\left[\rho_D\left(E_D^n + \frac{w_1}{2}\right) - (\alpha_1 + m_D)\left(R_D^n + \frac{n_1}{2}\right)\right],\\
o_2 &= h\left[B_H + \gamma_H\left(R_H^n + \frac{j_1}{2}\right) - \left(m_H + \beta_{DH}\left(I_D^n + \frac{m_1}{2}\right)\right)\right.\\
&\left.\left(S_H^n + \frac{o_1}{2}\right)\right],\\
p_2 &= h\left[\beta_{DH}\left(S_H^n + \frac{o_1}{2}\right)\left(I_D^n + \frac{m_1}{2}\right) - (m_H + \rho_H + (1-\rho_H)\delta_H)\right.\\
&\left.\left(E_H^n + \frac{p_1}{2}\right)\right],\\
q_2 &= h\left[(1-\rho_H)\delta_H\left(E_H^n + \frac{p_1}{2}\right) - (\mu_H + m_H)\left(I_H^n + \frac{q_1}{2}\right)\right],\\
j_2 &= h\left[\rho_H\left(E_H^n + \frac{p_1}{2}\right) - (\mu_H + \gamma_H)\left(R_H^n + \frac{j_1}{2}\right)\right].
\end{aligned}
$$

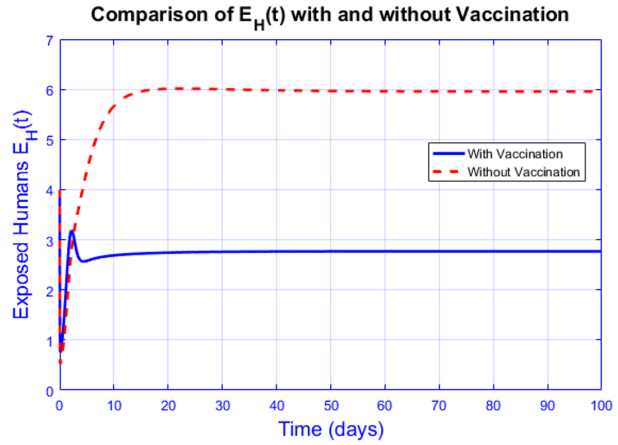

(a)

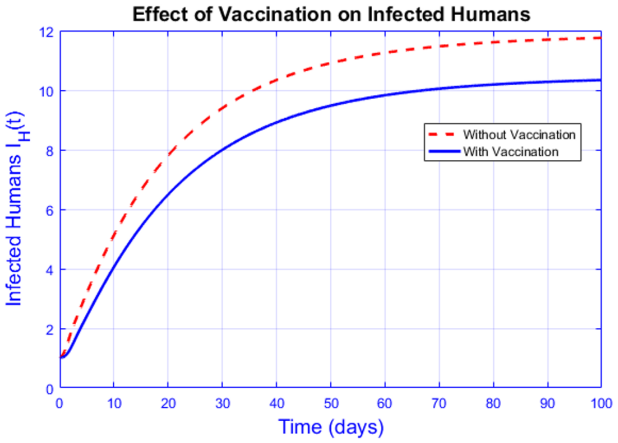

(b)

Figure 7. Human exposed (E_H) and infected (I_H) populations with and without vaccination: (a) exposed E_H and (b) infected I_H.

where $W_1 = \left(S_D^n + \frac{k_1}{2}\right)$

$$k_3 = h\left[A_D + \alpha_1\left(R_D^n + \frac{n_2}{2}\right) - \left(m_D + \beta_D\left(I_D^n + \frac{m_2}{2}\right)\right)\left(S_D^n + \frac{k_2}{2}\right)\right],$$

$$w_3 = h\left[\beta_D\left(I_D^n + \frac{m_2}{2}\right)\left(S_D^n + \frac{k_2}{2}\right) - (\delta_D + \rho_D + m_D + C_D)\left(E_D^n + \frac{w_2}{2}\right)\right],$$

$$m_3 = h\left[\delta_D\left(E_D^n + \frac{w_2}{2}\right) - (\mu_D + m_D)\left(I_D^n + \frac{m_2}{2}\right)\right],$$

$$n_3 = h\left[\rho_D\left(E_D^n + \frac{w_2}{2}\right) - (\alpha_1 + m_D)\left(R_D^n + \frac{n_2}{2}\right)\right],$$

$$o_3 = h\left[B_H + \gamma_H\left(R_H^n + \frac{j_2}{2}\right) - \left(m_H + \beta_{DH}(I_D^n + \frac{m_2}{2})\left(S_H^n + \frac{o_2}{2}\right)\right)\right],$$

$$p_3 = h\left[\beta_{DH}\left(S_H^n + \frac{o_2}{2}\right)\left(I_D^n + \frac{m_2}{2}\right) - (m_H + \rho_H + (1-\rho_H)\delta_H)\left(E_H^n + \frac{p_2}{2}\right)\right],$$

$$q_3 = h\left[(1-\rho_H)\delta_H\left(E_H^n + \frac{p_2}{2}\right) - (\mu_H + m_H)\left(I_H^n + \frac{q_2}{2}\right)\right],$$

$$j_3 = h\left[\rho_H\left(E_H^n + \frac{p_2}{2}\right) - (\mu_H + \gamma_H)\left(R_H^n + \frac{j_2}{2}\right)\right].$$

$$k_4 = h\Big[A_D + \alpha_1(R_D^n + n_3) - (m_D + \beta_D(I_D^n + m_3))\,(S_D^n + k_3)\Big],$$

$$w_4 = h\Big[\beta_D(I_D^n + m_3)(S_D^n + k_3) - (\delta_D + \rho_D + m_D + C_D)(E_D^n + w_3)\Big],$$

$$m_4 = h\Big[\delta_D(E_D^n + w_3) - (\mu_D + m_D)(I_D^n + m_3)\Big],$$

$$n_4 = h\Big[\rho_D(E_D^n + w_3) - (\alpha_1 + m_D)(R_D^n + n_3)\Big],$$

$$o_4 = h\Big[B_H + \gamma_H(R_H^n + j_3) - (m_H + \beta_{DH}(I_D^n + m_3))\,(S_H^n + o_3)\Big],$$

$$p_4 = h\Big[\beta_{DH}(S_H^n + o_3)(I_D^n + m_3) - (m_H + \rho_H + (1-\rho_H)\delta_H)\,(E_H^n + p_3)\Big],$$

$$q_4 = h\Big[(1-\rho_H)\delta_H(E_H^n + p_3) - (\mu_H + m_H)(I_H^n + q_3)\Big],$$

$$j_4 = h\Big[\rho_H(E_H^n + p_3) - (\mu_H + \gamma_H)(R_H^n + j_3)\Big].$$

$$k_8 = h\Big[A_D + \alpha_1(R_D^n + n_7) - (m_D + \beta_D(I_D^n + m_7))\,(S_D^n + k_7)\Big],$$

$$w_8 = h\Big[\beta_D(I_D^n + m_7)(S_D^n + k_7) - (\delta_D + \rho_D + m_D + C_D)\,(E_D^n + w_7)\Big],$$

$$m_8 = h\Big[\delta_D(E_D^n + w_7) - (\mu_D + m_D)(I_D^n + m_7)\Big],$$

$$n_8 = h\Big[\rho_D(E_D^n + w_7) - (\alpha_1 + m_D)(R_D^n + n_7)\Big],$$

$$o_8 = h\Big[B_H + \gamma_H(R_H^n + j_7) - (m_H + \beta_{DH}(I_D^n + m_7))\,(S_H^n + o_7)\Big],$$

$$p_8 = h\Big[\beta_{DH}(S_H^n + o_7)(I_D^n + m_7) - (m_H + \rho_H + (1-\rho_H)\delta_H)(E_H^n + p_7)\Big],$$

$$q_8 = h\Big[(1-\rho_H)\delta_H(E_H^n + p_7) - (\mu_H + m_H)(I_H^n + q_7)\Big],$$

$$j_8 = h\Big[\rho_H(E_H^n + p_7) - (\mu_H + \gamma_H)(R_H^n + j_7)\Big].$$

10.2 NSFD Scheme

We introduce a trustworthy numerical method in this subsection, based on the Nonstandard Finite Difference (NSFD) scheme developed by Mickens [23]. This approach finds applications in many real-world problems in engineering and mathematics. For more NSFD applications, see [24].

$$S_D^{n+1} = \frac{S_D^n + h(A_D + \alpha_1 R_D^n)}{1 + m_D + \beta_D I_D^n}$$

$$E_D^{n+1} = \frac{E_D^n + h\beta_D I_D^n S_D^n}{1 + h(\delta_D + \rho_D + (m_D + C_D)E_D^n)}$$

$$I_D^{n+1} = \frac{I_D^n + h\delta_D E_D^n}{1 + \mu_D + m_D}$$

$$R_D^{n+1} = \frac{R_D^n + h\rho_D E_D^n}{1 + \alpha_1 + m_D}$$

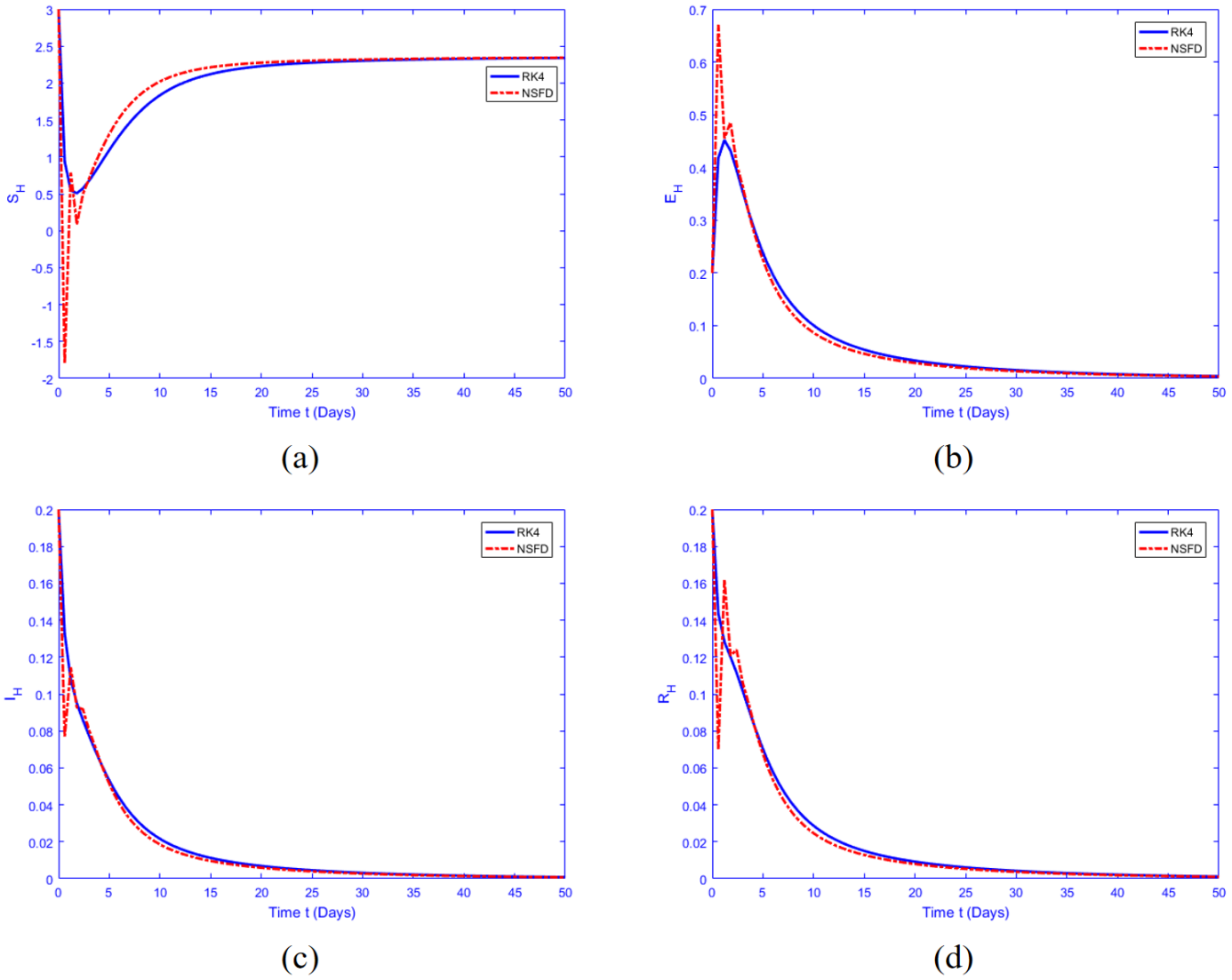

Figure 8. Comparison of solutions obtained by NSFD Method and RK-4 Method for F_0, with initial conditions $(S_H(0), E_H(0), I_H(0), R_H(0)) = (0.2, 0.2, 0.2, 0.2)$ and step size $h = 0.60$. Both methods converge to the true steady state of F_0 with $R_0 = 0.7120 < 1$.

$$S_H^{n+1} = \frac{S_H^n + hB_D + \gamma_H R_H^n}{1 + h(m_H + \beta_{DH} I_H^n)}$$

$$E_H^{n+1} = \frac{E_H^n + h\beta_{DH} S_H^n I_D^n}{1 + h(m_H + \rho_H + (1-\rho_H)\delta_H)}$$

$$I_H^{n+1} = \frac{I_H^n + h(1-\rho_H)\delta_H E_H^n}{1 + h(\mu_H + m_H)}$$

$$R_H^{n+1} = \frac{R_H^n + h\rho_H E_H^n}{1 + h(\mu_H + \gamma_H)}$$

Theorem: 5 *Equilibrium points of the continuous model (1): E_0, E_1 are maintained by the discrete model. Moreover, the stability behavior of the equilibrium points (and of the fixed points) of the NSFD scheme is the same.*

We make a comparison between the RK4 method and *NSFD* method with a discretization step size $h = 1.0$. The numerical methods are convergent and converge to the steady states E_0 and E_1 of the continuous model. With $h = 1.5$ and $R_0 < 1$, the RK4 method yields positive solutions; however, for larger values of h this may result in negative solutions. The NSFD method, however, always tends to positive solutions for both E_0 and E_1.

Figures 8 and 9 present a comparison between the *NSFD* (Nonstandard Finite Difference) method and the classical RK-4 (Runge-Kutta order 4) method in approximating the solution of the proposed rabies transmission model at the DFE F_0 with initial conditions $(S_H(0), E_H(0), I_H(0), R_H(0)) = (0.2, 0.2, 0.2, 0.2)$ and step size $h = 0.60$. Figure 8 shows the temporal evolution of the human population compartments: susceptible (S_H), exposed (E_H), infected (I_H), and partially immune (R_H)

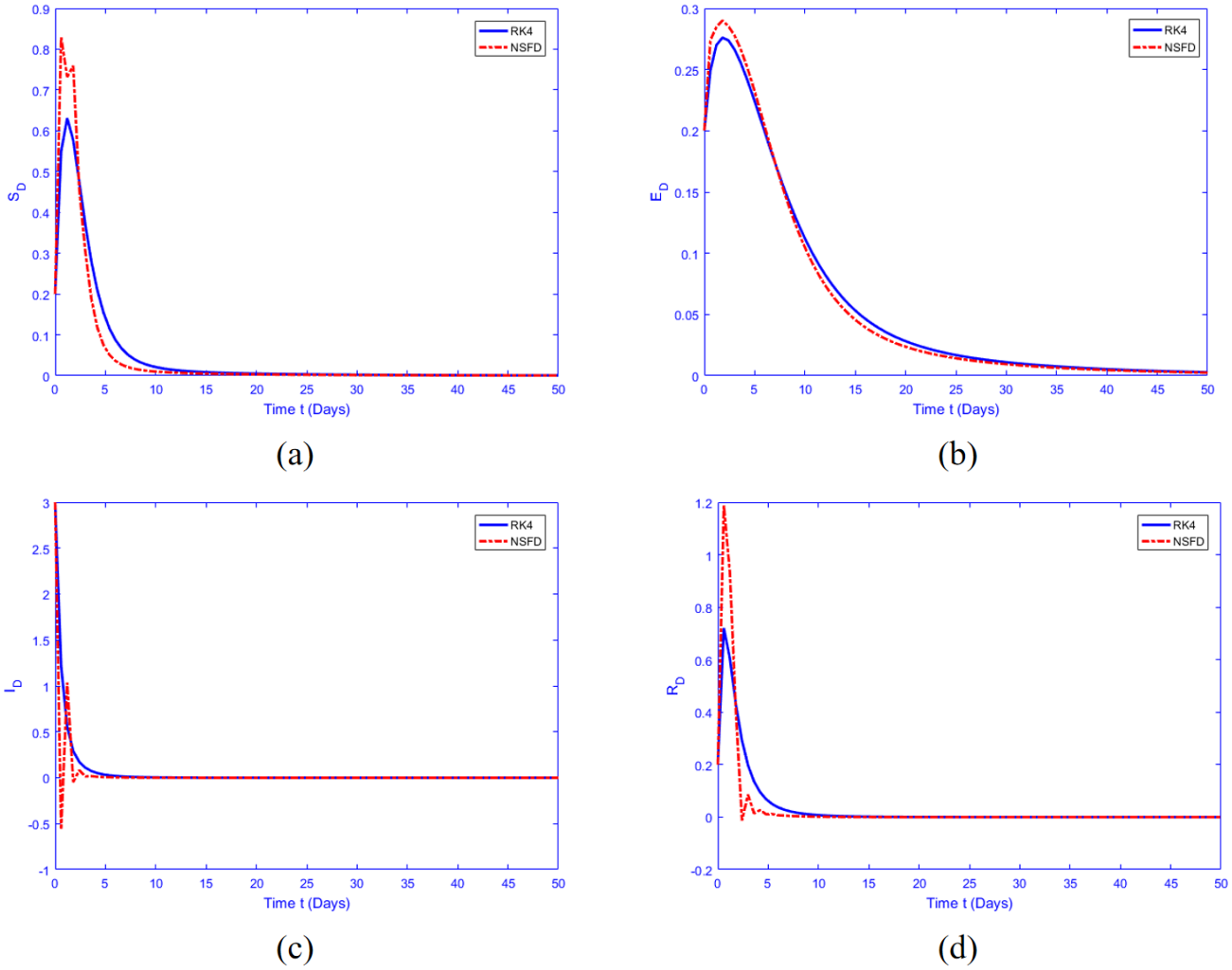

Figure 9. Comparison of solutions obtained by the NSFD and RK-4 methods for F_0, showing the dog population compartments: susceptible (S_D), exposed (E_D), infected (I_D), and partially immune (R_D), with initial conditions $(S_D(0), E_D(0), I_D(0), R_D(0)) = (0.2, 0.2, 0.2, 0.2)$ and step size $h = 0.60$. Both methods converge to the true steady state of F_0 with $R_0 = 0.7120 < 1$.

individuals. Both numerical schemes converge to the true steady state of F_0 as expected for $R_0 = 0.7120 < 1$, demonstrating the disease elimination scenario. Similarly, Figure 9 illustrates the corresponding dynamics for the dog population compartments: susceptible (S_D), exposed (E_D), infected (I_D), and partially immune (R_D). The NSFD method preserves positivity and stability throughout the simulation, whereas the RK-4 method shows conditional convergence dependent on the step size. These figures confirm the reliability and effectiveness of the NSFD scheme in capturing the model dynamics accurately while maintaining biologically meaningful solutions. In our numerical simulations, the effects of vaccination and infectious immigration are explicitly incorporated through the model parameters related to vaccination rates and immigrant inflow. Vaccination reduces the susceptible populations by moving individuals to the partially immune compartments, thereby decreasing the effective reproduction number R_0 and slowing the disease spread, as reflected in the stabilizing trends of the immune compartments shown in Figures 8 and 9. Infectious immigration, modeled as a constant influx of infected individuals into the population, sustains disease prevalence even when local transmission is controlled, highlighting the importance of monitoring and managing external sources of infection. Both RK4 and NSFD schemes successfully capture these dynamics, but the NSFD method consistently preserves the positivity and boundedness of all compartments, ensuring biologically realistic numerical solutions in

the presence of vaccination and immigration factors.

11 Conclusions

This study proposes a mathematical model of rabies transmission with eight compartments: susceptible, exposed, infected, and recovered compartments for dogs (S_D, E_D, I_D, R_D) as well as for humans (S_H, E_H, I_H, R_H). The basic reproduction number R_0 is derived and analyzed to see how sensitive it is to the main parameters, including the disease and transmission parameters. The disease-free equilibrium is analyzed for stability to gain insight into when rabies can be eradicated from the population. One of the major objectives of the study is the contrast of disease dynamics and without the vaccination interventions. The results of the simulations are presented graphically and demonstrate the dynamics of the infected and susceptible populations in both scenarios, emphasizing the ability of vaccination to manage rabies. Numerical simulation is carried out by the fourth-order Runge-Kutta (RK4) method and the nonstandard finite difference (NSFD) method and their performances are compared to check the accuracy and consistency. Moreover, the effect of the dog-to-human transmission rate parameter changing from $\beta_{DH} = 0.5$ to $\beta_{DH} = 2.5$ is investigated to study the effect of this parameter on the human infection burden. The results highlight the importance of vaccination and sensitivity of parameters in developing rabies control strategies.

Data Availability Statement

Data will be made available on request.

Funding

This work was supported without any funding.

Conflicts of Interest

The authors declare no conflicts of interest.

AI Use Statement

The authors declare that no generative AI was used in the preparation of this manuscript.

Ethical Approval and Consent to Participate

Not applicable.

References

[1] Younas, H., Ahmad, I., Ali, N., Haq, I. U., Albalwi, M. D., Muhammad, S., Shuaib, S., & Muhammad, M. (2024). Modeling rabies dynamics: The impact of vaccination and infectious immigrants on public health. *Contemporary Mathematics*, 3255-3279. [CrossRef]

[2] WHO Rabies Modelling Consortium. (2020). Zero human deaths from dog-mediated rabies by 2030: perspectives from quantitative and mathematical modelling. *Gates Open Research, 3*, 1564. [CrossRef]

[3] Hankins, D. G., & Rosekrans, J. A. (2004). Overview, prevention, and treatment of rabies. *Mayo Clinic Proceedings, 79*(5), 671-676. [CrossRef]

[4] Demirci, E. (2014). A new mathematical approach for rabies endemy. *Applied Mathematical Sciences, 8*(2), 59-67. [CrossRef]

[5] Layan, M., Dellicour, S., Baele, G., Cauchemez, S., & Bourhy, H. (2021). Mathematical modelling and phylodynamics for the study of dog rabies dynamics and control: A scoping review. *PLOS Neglected Tropical Diseases, 15*(5), e0009449. [CrossRef]

[6] Jehangir, H., Ali, N., Ahmad, I., Younas, H., Ahmad, Z., & El-Agamy, R. F. (2024). Global dynamics and numerical simulation of a vaccinated mathematical model for rabies disease. *Global Journal of Sciences, 1*(1), 14-27. [CrossRef]

[7] Hailemichael, D. D., Edessa, G. K., & Koya, P. R. (2023). Mathematical modeling of dog rabies transmission dynamics using optimal control analysis. *Contemporary Mathematics*, 296-319. [CrossRef]

[8] Charles, M., Masanja, V. G., Torres, D. F., Mfinanga, S. G., & Lyakurwa, G. A. (2024). Mathematical model to assess the impact of contact rate and environment factor on transmission dynamics of rabies in humans and dogs. *Heliyon, 10*(11). [CrossRef]

[9] Zarin, R., Raouf, A., Humphries, U. W., & Khan, A. (2023). Numerical solutions of fractional order rabies mathematical model via Newton polynomial. *Alexandria Engineering Journal, 77*, 419-434. [CrossRef]

[10] Abdulmajid, S., & Hassan, A. S. (2021). Analysis of time delayed rabies model in human and dog populations with controls. *Afrika Matematika, 32*(5), 1067-1085. [CrossRef]

[11] Panjeti, V. G., & Real, L. A. (2011). Mathematical models for rabies. *Advances in Virus Research, 79*, 377-395. [CrossRef]

[12] Huang, Y., & Li, M. (2020). Application of a mathematical model in determining the spread of the rabies virus: Simulation study. *JMIR Medical Informatics, 8*(5), e18627. [CrossRef]

[13] Kadowaki, H., Hampson, K., Tojinbara, K., Yamada, A., & Makita, K. (2018). The risk of rabies spread in Japan: A mathematical modelling assessment. *Epidemiology and Infection, 146*(10), 1245-1252. [CrossRef]

[14] Jothi, N. K., Muruganandham, A., Kumar, P. S., & Dayalan, S. K. (2025). Modeling rabies transmission dynamics with fractional order analysis: Examining stability, susceptibility, and vaccination impact. *AIP Advances, 15*(5). [CrossRef]

[15] Sinan, M., & Khan, A. (2020). Analytic approximate solution of rabies transmission dynamics using homotopy perturbation method. *Matrix Science Mathematics (MSMK), 4*(1), 01-05. [CrossRef]

[16] Pantha, B., Joshi, H. R., & Vaidya, N. K. (2020). Controlling rabies epidemics in Nepal with limited resources: Optimal control theory approach. *Mathematics in Applied Sciences and Engineering, 1*(4). [CrossRef]

[17] Zhang, J., Jin, Z., Sun, G. Q., Zhou, T., & Ruan, S. (2011). Analysis of rabies in China: transmission dynamics and control. *PLoS one, 6*(7), e20891. [CrossRef]

[18] Hampson, K., Dushoff, J., Cleaveland, S., Haydon, D. T., Kaare, M., Packer, C., & Dobson, A. (2009). Transmission dynamics and prospects for the elimination of canine rabies. *PLoS biology, 7*(3), e1000053. [CrossRef]

[19] Minghui, R., Stone, M., Semedo, M. H., & Nel, L. (2018). New global strategic plan to eliminate dog-mediated rabies by 2030. *The Lancet global health, 6*(8), e828-e829. [CrossRef]

[20] Van den Driessche, P., & Watmough, J. (2002). Reproduction numbers and sub-threshold endemic equilibria for compartmental models of disease transmission. *Mathematical biosciences, 180*(1-2), 29-48. [CrossRef]

[21] Chitnis, N., Hyman, J. M., & Cushing, J. M. (2008). Determining important parameters in the spread of malaria through the sensitivity analysis of a mathematical model. *Bulletin of mathematical biology, 70*(5), 1272-1296. [CrossRef]

[22] Castillo-Chavez, C., & Song, B. (2004). Dynamical models of tuberculosis and their applications. *Mathematical biosciences and engineering, 1*(2), 361. https://www.aimspress.com/aimspress-data/mbe/2004/2/PDF/1551-0018_2004_2_361.pdf

[23] Mickens, R. E. (Ed.). (1993). *Nonstandard finite difference models of differential equations*. World scientific. [CrossRef]

[24] Mehdizadeh Khalsaraei, M., Shokri, A., Noeiaghdam, S., & Molayi, M. (2021). Nonstandard finite difference schemes for an SIR epidemic model. *Mathematics, 9*(23), 3082. [CrossRef]

Hazrat Younas received his M.Phil. degree in Mathematics from the University of Malakand, Khyber Pakhtunkhwa, Pakistan, in 2024. His academic interests include applied mathematics and mathematical modeling. (Email: mathskhan18@gmail.com)

Imtiaz Ahmad is a Professor and Chairman of the Department of Mathematics at the University of Malakand, Khyber Pakhtunkhwa, Pakistan. His academic and research interests include mathematics and related areas of applied mathematical research. (Email: iahmaad@hotmail.com)

Naseer Ul Haq received his M.Phil. degree in Mathematics from the University of Malakand, Khyber Pakhtunkhwa, Pakistan, in 2025. His academic interests include mathematics and applied mathematical research. (Email: naseerlhaqpk100@gmail.com)

Azizur Rahman received his M.Sc. degree in Mathematics from the University of Malakand, Khyber Pakhtunkhwa, Pakistan, in 2018. His academic interests include mathematics and mathematical research. (Email: azizmaths7@gmail.com)

Hanif Ullah received his M.Sc. degree in Mathematics from the University of Malakand, Khyber Pakhtunkhwa, Pakistan, in 2018. His academic interests include mathematics and applied mathematical research. (Email: azizmaths7@gmail.com)